Graphite under pressure: Equation of state and first-order Raman modes

M. Hanfland, H. Beister, and K. Syassen
Max-Planck-Institut für Festkörperforschung, D-7000 Stuttgart 80, Federal Republic of Germany
(Received 3 October 1988)

We have measured lattice parameters and Raman spectra of hexagonal graphite at pressures up to the structural phase transition near 14 GPa ($T=300$ K). The frequencies of the $E_{2g}(1)$ rigid-layer shear mode at 44 cm^{-1} and the $E_{2g}(2)$ in-plane mode at 1579 cm^{-1} increase sublinearly under pressure with initial pressure coefficients of 4.8(5) and 4.7(3) cm^{-1}/GPa, respectively. Using the a- and c-axis compression data, we determine the dependence of phonon frequencies on intralayer and interlayer separation. For the high-frequency $E_{2g}(2)$ mode we find $d\ln\omega/3\,d\ln a=1.06(10)$, which is in the range of bond-length scaling parameters of phonon frequencies in three-dimensional covalent structures. For the low-frequency $E_{2g}(1)$ mode we obtain $d\ln\omega/3d\ln c=1.4(1)$, which indicates a stronger anharmonicity of this mode.

I. INTRODUCTION

A unique property of graphite is its high degree of structural anisotropy. Within the two-dimensional hexagonal lattice of the graphite basal plane, the carbon atoms are held together by strong covalent bonds, whereas the bonding between adjacent planes is much weaker resulting in a large interlayer distance (3.35 Å), as compared with the in-plane nearest-neighbor separation (1.42 Å). The strong anisotropy of the bonding is clearly reflected in the elastic and vibrational properties of graphite. Phonons and elastic properties of hexagonal graphite at normal pressure have been thoroughly investigated[1] by Raman scattering,[2–4] infrared reflectance,[3,5] inelastic neutron scattering,[6] and elastic constant measurements.[7] Various lattice-dynamical models have been developed to account for the experimental phonon dispersion relations.[1,8] The Raman-active zone-center modes of hexagonal graphite ($ABAB\cdots$ layer sequence, 4 atoms per unit cell) consist of two E_{2g} modes, a rigid-layer shear mode near 42 cm^{-1} [$E_{2g}(1)$], and a high-frequency mode at about 1581 cm^{-1} [$E_{2g}(2)$] which involves in-plane displacements.[2–4] For schematic representations of the atomic displacements of all zone-center modes of graphite we refer to Refs. 1 and 5.

Here we report on the effect of hydrostatic pressure on first-order Raman spectra and lattice parameters of graphite. Raman measurements and powder x-ray diffraction studies were performed at 300 K by using a diamond window pressure cell[9] in combination with the ruby luminescence method for pressure determination.[10] The primary motivation for this investigation was to study vibrational modes of this prototype of a layered material over an extended range of pressure ($P\leq 14$ GPa) and as a function of intralayer and interlayer atomic distances. In particular, we are interested in comparing the dependence of the $E_{2g}(2)$ mode frequency on in-plane lattice parameter with the mode Grüneisen parameter of the Raman-active zone-center modes of diamond which is the prototype of a three-dimensional covalent material. Furthermore, a recent theoretical treatment[11] of the interlayer bonding predicts a strong anharmonicity of the low-frequency $E_{2g}(1)$ mode; this anharmonicity should manifest itself in a strong increase of the $E_{2g}(1)$ mode frequency with pressure and interlayer separation, as is also observed for low-frequency modes in other layer-type crystals under pressure.[12,13]

We have determined a- and c-axis lattice parameters under pressure in order to provide a firm and consistent basis for discussing the dependence of Raman mode frequencies on intralayer and interlayer atomic distances. A previous x-ray study of graphite by Lynch and Drickamer[14] covers the pressure range up to about 20 GPa, but is based on a different pressure scale. Furthermore, the initial a-axis compressibility obtained from the earlier x-ray study is about three times higher compared to the compressibility calculated from elastic constant data.[7] Thus, for our present purpose of investigating phonon frequencies as a function of atomic distances, there is clearly a need for an independent determination of the lattice parameters under pressure. We note that the equation of state of graphite is an important ingredient to theoretical descriptions of the phase diagram of carbon.[15,16] This aspect of the present results, however, will not be discussed in this paper.

The present study is limited in pressure to about 14 GPa, where the single crystalline graphite samples, as used in the Raman experiments, start to transform to a different phase of carbon.[17–19] To our knowledge, the structural properties of this high-pressure phase has not been characterized by *in situ* experiments. However, the sp^3-bonded hexagonal form of diamond (wurtzite analog or "lonsdalite") appears to be the most likely candidate, since this phase has been identified by x-ray diffraction in samples which were recovered from static high-pressure runs involving additional temperature treatment.[18]

II. LATTICE PARAMETERS UNDER PRESSURE

The powder samples used in x-ray diffraction measurements were prepared by grinding natural graphite flakes.[20] The zero-pressure lattice parameters are

$a_0=2.603(4)$ Å and $c_0=6.706(3)$ Å in agreement with the data reported in the literature[21] (throughout this paper the index zero refers, to ambient pressure). Samples were loaded into the diamond anvil cell using a 4:1 methanol-ethanol pressure medium. High-pressure x-ray-diffraction spectra were measured in the angle-dispersive mode using filtered Mo $K\alpha$ radiation and a position-sensitive proportional counter. The a- and c-axis lattice parameters under pressure were determined from the (100), (002), and (101) Bragg reflections. Above about 14 GPa these Bragg reflections could not be observed. This is attributed to the transformation to the high-pressure phase of carbon. The poor quality of the x-ray-diffraction pattern above 14 GPa did not allow for an identification of the crystal structure of this phase.

Figure 1 shows the normalized lattice parameters a/a_0 and c/c_0 of graphite as a function of pressure. The one-dimensional analog of the Murnaghan equation[22] provides an approximation for describing the nonlinear relation between normalized lattice parameters and pressure P,

$$r/r_0=[(\beta'/\beta_0)P+1]^{-1/\beta'} . \quad (1)$$

Here, r is the lattice constant along one of the crystal axes, $\beta_0^{-1}=-(d\ln r/dP)_{P=0}$ is the linear compressibility, and β' is the pressure derivative of β. The solid lines in Fig. 1 correspond to Eq. (1) with parameters obtained from a least-squares fit to the experimental data. The dashed lines in Fig. 1 represent the results of Ref. 14. The parameters β_0 and β' are listed in Table I. In the case of the a axis, we have only determined an *average* modulus for the pressure range covered in this experiment ($\beta'=1$), because the pressure-induced change is extremely small and, therefore, the relative scatter of the experimental data is large.

The modulus $\beta_0(c)$ along the c axis is in good agreement with previous results from x-ray measurements using powder samples[14,23] and single crystals,[24] and also with the adiabatic values derived from the measured elastic constants.[7,25] The pressure derivative $\beta'(c)$ is smaller than that obtained from previous x-ray data.[14] This difference is at least partly due to the use of different pressure scales. The measured pressure dependence ($P<2$ GPa) of the elastic constant C_{33} yields $\beta'(c)=9.9$, 9.6, and 15 according to Refs. 25–27, respectively.

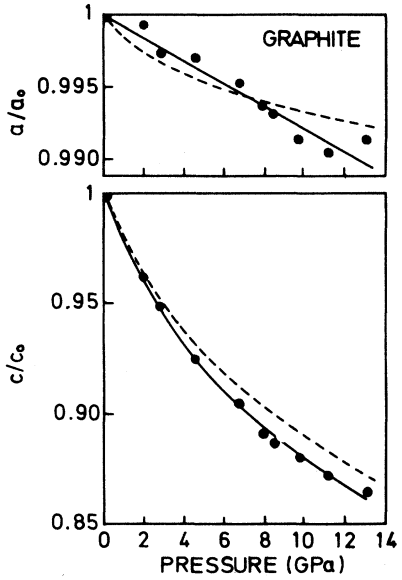

FIG. 1. Relative lattice parameters a/a_0 and c/c_0 of hexagonal graphite as a function of pressure. The solid line correspond to the result of a least-squares fit of Eq. (1) to the experimental data (full dots). Dashed lines represent results of Lynch and Drickamer (Ref. 14).

We find an average a-axis compressibility which is close to the compressibility of diamond [β_0(diamond)=1326 GPa, Ref. 28]. The a-axis modulus $\beta_0(a)$ calculated[29] from elastic constants of graphite (see Table I) is significantly higher than the present result for $\beta_0(a)$, whereas the previous x-ray-diffraction data[14] yielded a much lower value for $\beta_0(a)$ and a pronounced nonlinearity [large $\beta'(a)$] for the a-axis compression (see dashed line in Fig. 1). It has been suggested that the nonlinear behavior arises from the onset of buckling or puckering of the graphite layers at low pressures.[30] This interpretation, however, has been questioned in a later analysis of the earlier compression data using molecular force constants for C—C stretching and out-of-plane displacements.[31] Although the relative experimental errors in-

TABLE I. First- and second-order axial compression coefficients of graphite. β_0^{-1} is the linear compressibility at zero pressure and β' is the pressure derivative of β [see Eq. (1)].

	β_0 (GPa)	β'	Method
c axis	35.7(25)	10.8(9)	Present work
	35.0	14	x ray[a] ($P>15$ GPa)
	35.7,36.6		x ray[b,c] ($P\leq 1.6$ GPa)
	37.3,34.0		Elastic constants[d,e]
a axis	1250(70)	1[f]	Present work
	640	210	x ray[a]
	2000		Elastic constants[d]

[a]Reference 14.
[b]Reference 23.
[c]Reference 24.
[d]Reference 7.
[e]Reference 25.
[f]Fixed parameter.

volved in the determination of the a-axis compression are quite large, it is safe to conclude that the present results are not consistent with this pronounced nonlinearity. Hence, we find no indication for a significant puckering or buckling of the graphite layers during the initial compression. This is also consistent with the theoretical calculation of Fahy *et al.*[32] for rhombohedral graphite, where the out-of-plane displacement remains essentially zero during the initial compression and changes significantly only upon approaching the predicted phase transition from rhombohedral graphite to cubic diamond near 80 GPa.

Figure 2 shows the experimental equation of state of graphite at $T=300$ K. The volume at ambient pressure is $V_0=35.12(2)$ Å^3/unit cell. The solid line corresponds to the result of a least-squares fit to the experimental data using the Murnaghan equation. The bulk modulus $B=-dP/d\ln V$ and its pressure derivative at ambient pressure thus obtained are

$$B_0=33.8(30)\ \text{GPa}$$

and

$$B'=8.9(10)\ ,$$

respectively. The dashed line in Fig. 2 again represents the results of Ref. 14.

In the following discussion of Raman modes and their mode Grüneisen parameters, we will refer to our data (see Table I) for the a- and c-axis compression of graphite.

III. RAMAN MODES UNDER PRESSURE

For Raman measurements we have used single-crystalline graphite flakes,[20] which were cleaved to about 20-μm thickness and cut to about 100-μm edge length. A micro-optical system[33] in backscattering geometry was used to focus the exciting laser into the pressure cell and to collect the light scattered from the sample. Most of the low-frequency spectra in the range of the interlayer $E_{2g}(1)$ mode were measured with a soft solid pressure medium (KCl), such that the sample could be held in a fixed position as close as possible to the diamond window. This sample mounting allowed us to reduce background scattering arising from the thin layer of pressure medium between diamond window and sample. The spectra of this extremely weak shear mode were recorded using 514.5- or 632.8-nm excitation and a multichannel spectrometer system.[34] For measurements in the high-frequency range of the in-plane $E_{2g}(2)$ mode the samples were always immersed in a methanol-ethanol pressure medium and the spectra were recorded using 514.5-nm excitation, a conventional double grating spectrometer, and single-channel photon counting. In both experimental configurations the resolution was better than 5 cm^{-1}.

Raman spectra in the frequency ranges 20–200 cm^{-1} and 1500–1700 cm^{-1} are shown in Figs. 3 and 4, respectively. With the sample inside the pressure cell, a low-frequency Raman line could be observed only at pressures above ~4.5 GPa (see Fig. 3). It is obvious to associate this Raman line with the $E_{2g}(1)$ shear-type mode. The zero-pressure frequency of the $E_{2g}(1)$ mode measured for a free-standing sample is $\omega_0=44(1)$ cm^{-1} in close agreement with the value of 42(1) cm^{-1} reported by

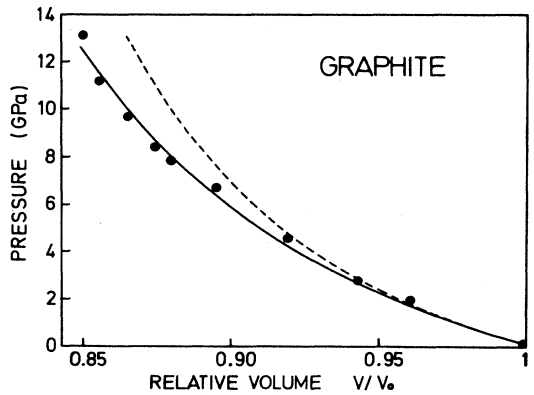

FIG. 2. Equation of state of graphite at 300 K. Solid dots are our experimental data. Solid line represents the result of a least-squares fit using a Murnaghan equation. Dashed line is from Ref. 14.

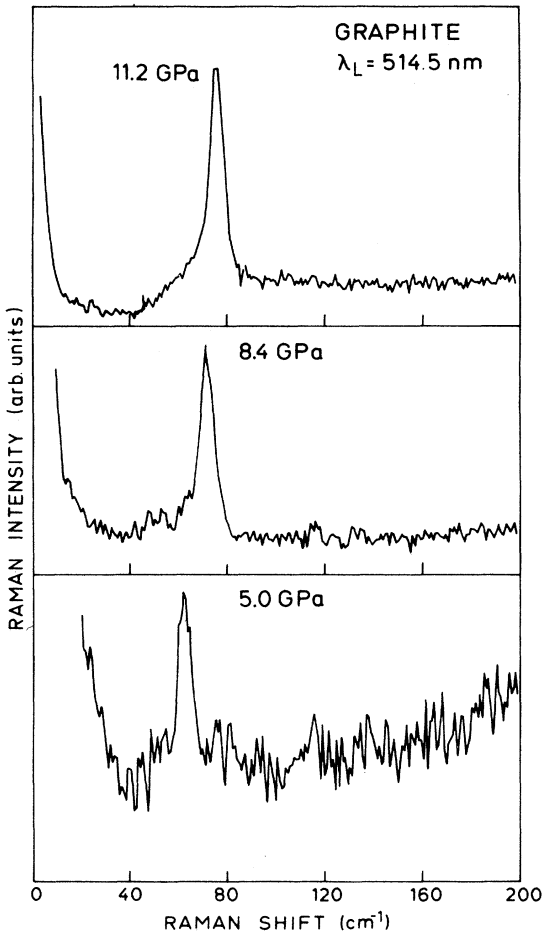

FIG. 3. Raman spectra of graphite at different pressures measured in the frequency range of the $E_{2g}(1)$ rigid-layer shear mode.

Nemanich *et al.*[4] The variation of the signal-to-noise ratio in Fig. 3 shows that the intensity of this line increases monotonically as pressure increases. The frequency of the $E_{2g}(2)$ mode at ambient pressure is observed at $\omega_0 = 1579(1)$ cm^{-1}. With increasing pressure, this line also shifts to higher frequency (see Fig. 4). The $E_{2g}(2)$ mode does not show any major change in intensity with increasing pressure (note that different levels of background have been subtracted from the spectra in Fig. 4).

No Raman signal could be observed at pressures above the onset of the phase transition at about 14 GPa, which in the case of single crystals is easily detected by visual observation.[35] At the transition to the sp^3-bonded hexagonal form of diamond, one would expect two Raman lines to appear. One line should be close to 1380 cm^{-1}, since this is the frequency of the Raman mode of cubic diamond at this pressure.[36] The second line would be expected at a frequency which is lower by about 100 cm^{-1} compared to the first one.[37] In the present experiment this frequency range is partly masked by the strong scattering from the diamond window of the pressure cell, which prevented us from detecting a Raman signal from the transformed sample in this frequency range.

The pressure dependence of the Raman linewidths is shown in Fig. 5. The width of the $E_{2g}(1)$ line remains essentially constant at about 8 cm^{-1}. Below about 10 GPa, the linewidth of the $E_{2g}(2)$ line is about 15 cm^{-1}; this linewidth increases significantly at higher pressures.

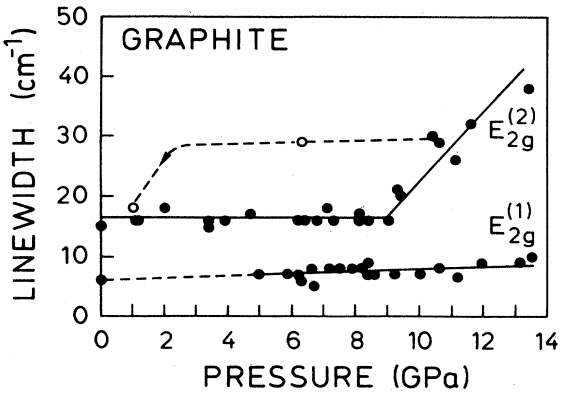

FIG. 5. Linewidth [full width at half maximum (FWHM)] of Raman modes of graphite as a function of pressure. Open circles and dashed lines are for decreasing pressure.

Figure 5 shows that the change in linewidth of the $E_{2g}(2)$ observed above 10 GPa shows a large hysteresis and is fully reversible only after releasing the pressure below roughly 3 GPa. This large hysteresis is similar to that observed for the changes in resistance[15] and reflectivity[35] at the phase transition. We thus favor an explanation where the increase in linewidth arises from the formation of sp^3 bonds upon approaching the phase transition.

Figure 6 shows the Raman shifts of the two E_{2g} modes of graphite as a function of pressure. Despite the extremely large difference in their frequencies, both modes

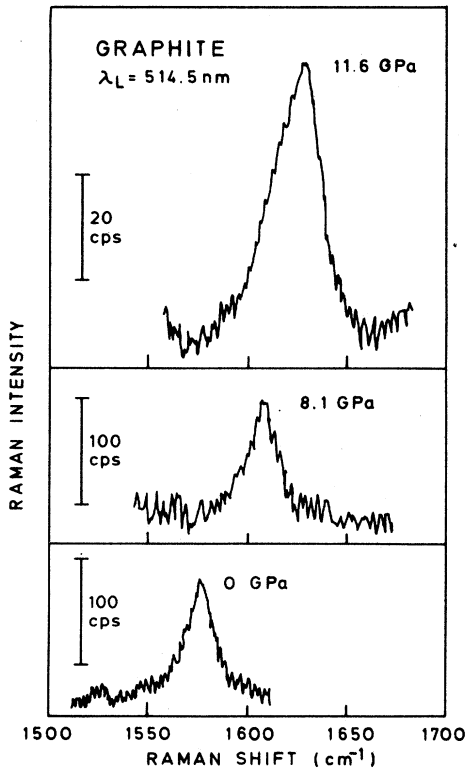

FIG. 4. Same as Fig. 3 for the $E_{2g}(2)$ high-frequency in-plane mode. Intensities (in counts per second) refer to a laser power of about 100 mW.

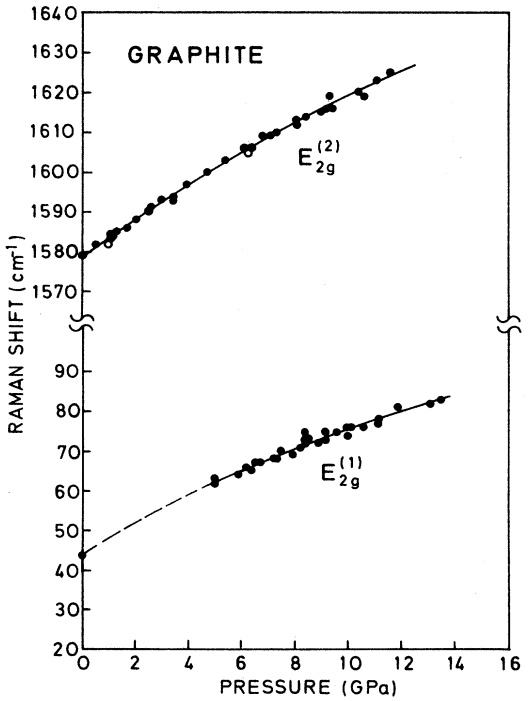

FIG. 6. Raman shifts of the two E_{2g} modes of graphite. Lines represent results of a least-squares fit of Eq. (2) to the experimental data. Open circles are for decreasing pressure.

show a very similar *absolute* shift with pressure. Furthermore, we observe a pronounced sublinear dependence on pressure for the two modes. Raman line frequencies are reversible upon decreasing the pressure. A least-squares fit of the relation

$$\omega(P)/\omega_0=[(\delta_0/\delta')P+1]^{\delta'} \quad (2)$$

to the experimental data yields the first- and second-order parameters δ_0 and δ' given in Table II. Here, δ_0 is the logarithmic pressure derivative $(d\ln\omega/dP)_{P=0}$ and δ' is the pressure derivative of $d\ln\omega/dP$. The corresponding absolute frequency shifts are $\delta_0\omega_0=4.8$ and 4.7 cm^{-1}/GPa for $E_{2g}(1)$ and $E_{2g}(2)$, respectively.

The mode Grüneisen parameter γ_G is commonly defined as[13]

$$\omega(P)/\omega_0=[V(P)/V_0]^{-\gamma_G} . \quad (3)$$

In the present case of a highly anisotropic crystal this Grüneisen scaling relation yields parameters γ_G which strongly vary with mode frequency, in contrast to what is usually observed for more isotropic materials.[13] The values for $\gamma_G=B_0\delta_0$ are 3.7 and 0.1 for the $E_{2g}(1)$ and $E_{2g}(2)$ modes of graphite, respectively. This large difference in the values of γ_G is similar to the case of molecular and other layered crystals,[12,13] where the mode frequencies usually separate into a low-frequency region for intermolecular modes with γ_G of order unity and a high-frequency region for intramolecular modes with $\gamma_G \ll 1$.

For an anisotropic hexagonal system two independent components of the Grüneisen tensor have been associated which each mode corresponding to the strain derivatives parallel $(\gamma_\parallel=-d\ln\omega/d\ln c)$ and perpendicular $[\gamma_\perp=-d\ln\omega/(2\,d\ln a)]$ to the c axis.[38] Instead of using the definitions of Ref. 38 for the Grüneisen tensor elements, we prefer here the scaling relation proposed by Zallen[22] with scaling parameter γ given by

$$\omega(P)/\omega_0=[r(P)/r_0]^{3\gamma} , \quad (4)$$

where r refers to the in-plane and out-of-phase lattice constants for intralayer and interlayer modes, respectively. The definitions Eqs. (3) and (4) are, of course, equivalent for three-dimensional isotropic materials.

For the high-frequency $E_{2g}(2)$ mode, the average value for the pressure range up to 14 GPa is $\bar{\gamma}_2=1.06(15)$, as determined from a least-squares fit of γ in Eq. (4) to the experimental data. Within experimental uncertainties this value agrees with the mode Grüneisen parameter of the first-order Raman mode of diamond ($\gamma=0.96$, Ref. 36). Thus, for the two-dimensional graphite layer we find a scaling parameter which is essentially identical to typical values[43] for optical phonons in the group-IV tetrahedral semiconductors.

A corresponding determination of $\bar{\gamma}$ for the low frequency $E_{2g}(1)$ yields $\bar{\gamma}_1=1.4(1)$. This value of $\bar{\gamma}_1$ is larger than $\bar{\gamma}_2$ indicating a larger relative change in force constants involved in the rigid-layer motion. A density functional study of the interplanar binding in graphite by DiVincenco *et al.*[11] predicts the frequency of the $E_{2g}(1)$ mode in close agreement with the experimental value. Furthermore, from their model the authors find the $E_{2g}(1)$ mode to be strongly anharmonic. It is true that the present results confirm a stronger anharmonicity of $E_{2g}(1)$ compared to $E_{2g}(2)$, but this difference is small relative to the range of magnitudes spanned by mode Grüneisen parameters in covalent and ionic materials.

Recently, the pressure dependence of the longitudinal optic $B_{1g}(1)$ mode of graphite ($\omega_0=127$ cm^{-1}) has been studied by inelastic neutron scattering up to 2 GPa.[25] A shift of 19 cm^{-1}/GPa has been observed for the $B_{1g}(1)$ mode. Thus, this mode exhibits an even larger logarithmic pressure dependence than the $E_{2g}(1)$ mode (see Table II).

Finally, we have checked the possibility that the increase in line intensity of the low-frequency $E_{2g}(1)$ mode is related to a resonance enhancement arising from a pressure-dependent change of the electronic excitation spectrum of graphite. By switching from green to red laser excitation we could not find a significant difference in line intensity at any pressure. Thus, the pressure-induced increase in line intensity is not caused by a *narrow* resonance. On the other hand, recent optical reflectivity measurements of graphite under pressure[35] show that the A_2 interband transition[39] shifts from about 0.8 eV at ambient pressure to 1.8 eV at 12 GPa. Hence, electronic excitations of graphite are strongly pressure dependent, and these effects may be responsible for a pressure-enhanced resonance effect which is active over a fairly broad spectral range of the exciting laser line. Other possibilities to explain the increase in line intensity include an increase of the Raman cross section due to a stronger interlayer coupling under pressure.

TABLE II. Zone-center phonons of graphite and their pressure dependence. ω_0 is the phonon frequency at ambient pressure, δ_0 is the logarithmic pressure derivative $(d\ln\omega/dP)_{P=0}$, and δ' is the pressure derivative of $d\ln\omega/dP$ [see Eq. (2)]; $\bar{\gamma}$ refers to the average scaling parameter $\gamma=-d\ln\omega/(3\,d\ln r)$ (see text for details).

Mode	ω_0 (cm^{-1})	δ_0 (GPa^{-1})	δ'	$\bar{\gamma}$
$E_{2g}(1)$	44(1)	0.110(8)	0.43(3)	1.4(1)
$B_{1g}(1)$	127[a]	0.15[a]		
$E_{2g}(2)$	1579(1)	$2.96(2)\times10^{-3}$	0.080(5)	1.06(0)

[a]Reference 25.

IV. CONCLUSIONS

We have measured the change of lattice parameters and the shift of the two Raman-active modes of hexagonal graphite at pressures up to about 14 GPa, which corresponds to the stability range for single-crystalline graphite samples. Within experimental uncertainty, the a-axis compression $\Delta a/a_0$ is essentially linear in pressure and does not confirm the strong nonlinearity found in previous x-ray diffraction experiments.[14] Based on the pressure dependence of the Raman frequencies of the E_{2g} modes, the mode Grüneisen parameters have been evaluated using the present compressibility data. The average scaling parameter $\bar{\gamma}_2 = d \ln \omega / (3\, d \ln a)$ [see Eq. (4)], corresponding to the pressure dependence of the $E_{2g}(2)$ in-plane mode, is close to unity and thus almost identical to that of the Raman mode of cubic diamond which can be viewed as the prototype of a three-dimensional covalent system. The scaling parameter $\bar{\gamma}_1 = d \ln \omega / (3d \ln c)$ for the $E_{2g}(1)$ rigid-layer shear mode is larger compared to $\bar{\gamma}_2$ thus indicating a stronger anharmonicity of this mode, in agreement with the qualitative prediction of DiVincenco *et al.*[11]

ACKNOWLEDGMENTS

We would like to thank O. H. Nielsen for communicating unpublished results of a first-principles calculation of the zone-center splitting of optical-phonon modes in hexagonal diamond. We gratefully acknowledge the technical assistance of W. Böhringer and W. Dieterich.

[1]For a brief review see M. S. Dresselhaus and G. Dresselhaus, in *Light Scattering in Solids,* edited by M. Cardona and G. Güntherodt (Springer, Berlin, 1982), Vol. III, p. 3.
[2]F. Tuinstra and J. L. Koenig, J. Chem. Phys. **53**, 1126 (1970).
[3]L. J. Brillson, E. Burstein, A. A. Maradudin, and T. Stark, in *Semimetals and Narrow Gap Semiconductors,* edited by D. L. Cartar and R. T. Bate (Pergamon, New York, 1971), p. 187.
[4]R. J. Nemanich, G. Lucovsky, and S. A. Solin, in *Proceedings of the International Conference on Lattice Dynamics,* edited by M. Balkanski (Flammarion, Paris, 1975), p. 619.
[5]R. J. Nemanich, G. Lucovsky, and S. A. Solin, Solid State Commun. **23**, 117 (1977).
[6]R. Nicklow, N. Wakabayashi, and H. G. Smith, Phys. Rev. B **5**, 4951 (1972).
[7]O. L. Blakslee, D. G. Proctor, E. J. Seldin, G. B. Spence, and T. Weng, J. Appl. Phys. **41**, 3373 (1970); E. Seldin and C. W. Nezbeda, *ibid.* **41**, 3389 (1970).
[8]R. Al-Jishi and G. Dresselhaus, Phys. Rev. B **26**, 4514 (1982), and references therein.
[9]G. Huber, K. Syassen, and W. B. Holzapfel, Phys. Rev. B **15**, 5123 (1977); A. Jayaraman, Rev. Mod. Phys. **55**, 65 (1983).
[10]H. K. Mao, P. M. Bell, J. Shaner, and D. Steinberg, J. Appl. Phys. **49**, 3276 (1978).
[11]D. P. DiVincenco, E. J. Mele, and N. A. W. Holzwarth, Phys. Rev. B **27**, 2458 (1983).
[12]R. Zallen, Phys. Rev. B **9**, 4485 (1974).
[13]B. Weinstein and R. Zallen, in *Light Scattering in Solids,* edited by M. Cardona and G. Güntherodt (Springer, Berlin, 1984), Vol. IV.
[14]R. W. Lynch and H. G. Drickamer, J. Chem. Phys. **44**, 181 (1966).
[15]P. Gustafson, Carbon **24**, 169 (1986).
[16]M. van Thiel and F. H. Ree (unpublished).
[17]R. B. Aust and H. G. Drickamer, Science **140**, 817 (1963).
[18]F. Bundy and J. S. Kasper, J. Chem. Phys. **46**, 3437 (1967).
[19]For a recent review see R. Clarke and C. Uher, Adv. Phys. **33**, 469 (1984).
[20]We have used purified graphite flakes supplied by Graphitwerk Kropfmühl AG, München, Federal Republic of Germany.
[21]J. Donohue, *The Structure of the Elements* (Wiley, New York, 1974).
[22]F. D. Murnaghan, Proc. Natl. Acad. Sci. **30**, 244 (1944).
[23]S. S. Kabalkina and L. F. Vereshchagin, Sov. Phys.—Dokl. **5**, 373 (1960) [Dokl. Akad. Nauk SSSR **131**, 300 (1960)].
[24]N. Wada, R. Clarke, and S. A. Solin, Solid State Commun. **35**, 675 (1980).
[25]B. Alzyab, C. H. Perry, C. Zahopoulos, O. A. Pringle, and R. M. Nicklow, Phys. Rev. B **38**, 1544 (1988).
[26]W. B. Gauster and I. J. Fritz, J. Appl. Phys. **45**, 3309 (1974).
[27]J. F. Green, P. Bolsaitis, and I. L. Spain, J. Phys. Chem. Solids **34**, 1927 (1973).
[28]M. H. Grimsditch and A. K. Ramdas, Phys. Rev. B **11**, 3139 (1975).
[29]J. F. Nye, *The Physical Properties of Crystals* (Clarendon, Oxford, 1972).
[30]H. G. Drickamer, R. W. Lynch, R. L. Clarendon, and E. A. Perez-Albuerne, Solid State Phys. **19**, 135 (1966).
[31]J. R. Ritter, Jr., J. Chem. Phys. **52**, 5008 (1970).
[32]S. Fahy, S. G. Louie, and M. L. Cohen, Phys. Rev. B **34**, 1191 (1986).
[33]K. Syassen and R. Sonnenschein, Rev. Sci. Instrum. **53**, 633 (1982).
[34]Triplemate (Spex Industries, Edison, New Jersey) combined with Mepsicron photomultiplier (ITT, Fort Wayne, Indiana).
[35]M. Hanfland, R. Sonnenschein, and K. Syassen (unpublished).
[36]M. Hanfland, K. Syassen, S. Fahy, S. G. Louie, and M. L. Cohen, Phys. Rev. B **31**, 6896 (1985).
[37]O. H. Nielsen (private communication). The splitting of the zero-center modes of hexagonal diamond was calculated from a first-principles approach similar to that used in O. H. Nielson, Phys. Rev. B **34**, 5808 (1986).
[38]T. K. H. Barron and R. W. Munn, Philos. Mag. **15**, 85 (1967).
[39]A. Misu, E. E. Mendez, and M. S. Dresselhaus, J. Phys. Soc. Jpn. **47**, 199 (1979), and references therein.